

CHAPTER III

CALCULATION BASIS

3.1 Cryogenic System Definition

Originally, cryogenics referred to the technology and art of producing low temperatures (from the Greek words *kruos* for frost and *genos* for origin or creation). Today, cryogenics has come to describe the study of phenomena, techniques and concepts occurring at or pertaining to temperatures below 120 K. Thus, cryogenics deals with temperatures that cannot be usually observed on or near the Earth under natural conditions. The position and range of the field of cryogenics are illustrated on a logarithmic thermometer in Figure 3.1.

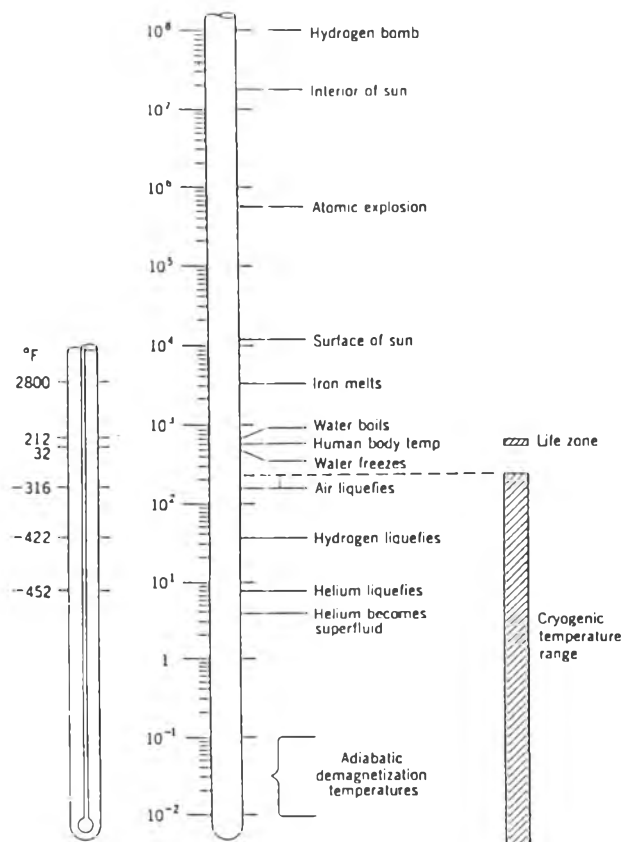


Figure 3.1 The cryogenic temperature range

It is important to note that although the origins of cryogenics are associated with very low temperatures, liquefaction of permanent gases and, ultimately, the quest for absolute zero, modern cryogenic technology is concerned with cooling and refrigeration systems at all temperatures below ambient.

In the field of cryogenic engineering, one is concerned with developing and improving low-temperature techniques, processes, and equipment. As contrasted to low-temperature physics, cryogenic engineering primarily involves the practical utilization of low-temperature phenomena, rather than basic research, although the dividing line between the two fields is not always clear-cut.

A system may be defined as a collection of components united by definite interactions or interdependencies in order to perform a definite function. In general, we shall use the term cryogenic system to refer to an interacting group of components involving low temperatures. Air-liquefaction plants, helium refrigerators, piping and storage vessels with associated controls are some examples of cryogenic systems.

The analysis and design of cryogenic systems is based on fundamental physical laws. For these laws to be applicable, we must above all choose a representative thermodynamic system isolated from its surroundings by a thermodynamic boundary. Such a system may be any macroscopic object of study, say a cryogenic apparatus or any part thereof or a machine or its part, etc. A thermodynamic system may or may not exchange mass and energy with its surroundings across the boundary, and external forces may be applied to the boundary. The system boundary may be treated as being rigid (as exemplified by mechanical insulation or processes at constant volume) or as perfectly elastic (as exemplified by processes at constant pressure). The boundary may be imparted the properties of an ideal thermal insulation (as in adiabatic systems), or any other qualities

3.2 The Properties of Cryogenic Fluids

Physical and thermodynamic properties of cryogenic fluids constitute important data that are needed for the design of cryogenic piping systems. Table 3.1 summarizes some of the more important properties for a number of cryogenic fluids. The cryogenic region of this application is characterized principally by three fluids: nitrogen, oxygen and argon.

3.2.1 Properties of Particular Cryogenes

Cryogenes are the liquid, or under appropriate conditions solid, form of substances more usually encountered as a gas and characterized by their extremely low boiling points.

1. Nitrogen

Liquid nitrogen is a clear, colorless fluid, which resembles water in appearance. At one atm pressure liquid nitrogen boils at 77.4 K and freezes at 63.2 K. Liquid nitrogen is widely used as cold source.

Nitrogen is present in the atmosphere at a concentration of 78.1 percent by volume or 75.5 percent by weight and is produced commercially by distillation of liquid air. The saturated liquid nitrogen has a density less than that of water. Nitrogen is a gas in normal atmospheric conditions (15° C and 760 mm Hg). It is colorless, odorless and tasteless. It is nonflammable gas.

It is the main ingredient of atmospheric air. Nitrogen is incapable of maintaining respiration or combustion, but plays an essential role as an element of living matter (animal and plant), and participates in the complex natural process of transformation of matter.

Nitrogen is supplied either as a pressurized gas in cylinders, or as a liquid at low temperature, under its own vapor pressure. Although nitrogen is a physiologically inert,

nontoxic gas can present a safety hazard as an asphyxiant. This danger is not confined to nitrogen but may occur in any otherwise safe atmosphere where the oxygen level falls below 20% by volume.

2. Oxygen

Liquid oxygen has a characteristic blue color, which is thought to be caused either by the presence of the polymer or long-chain molecule O_4 or by the unpaired electrons that are responsible for paramagnetism in liquid oxygen. At 1 atm pressure liquid oxygen boils at 90.2 K and freezes at 54.4 K. Saturated liquid oxygen at 1 atm is more dense than water at 60°F. Liquid oxygen is slightly magnetic in contrast to the other cryogenic fluids, which are nonmagnetic.

Liquid oxygen is chemically reactive, especially with hydrocarbon materials. Because of its chemical activity, oxygen presents a safety problem in handling. Serious explosions have resulted from the combination of oxygen and hydrocarbon lubricants.

Oxygen with an atomic number of 16 has three stable isotopes of mass numbers 16, 17 and 18. The relative abundance of these three isotopes is 10,000:4:20.

Oxygen is a gas in normal atmospheric conditions (15°C and 760 mm Hg). Oxygen is indispensable for the maintenance of life and for combustion. It is colorless, odorless and tasteless.

It accounts for 20.94 percent by volume of the air we breathe. Oxygen-poor atmospheres (less than 17% oxygen by volume) cause serious damage, capable of leading to death by asphyxiation if the oxygen content becomes excessively low (less than 12% by volume).

Oxygen is a highly reactive gas, which combines directly with most elements to form oxides in accordance with temperature conditions. Hence certain elements like phosphorus and magnesium ignite spontaneously in oxygen (or in air), while noble metals are only slowly oxidized at very high temperatures.

Oxygen is manufactured in large quantities by distillation of liquid air and is shipped either as a gas under high pressure in cylinders, or as a liquid at low temperature under its own vapor pressure.

3. Argon

Liquid argon is a clear, colorless fluid with properties similar to those of liquid nitrogen. At one atm pressure liquid argon boils at 87.3 K and freezes at 83.9 K. Saturated liquid argon at one atm is more dense than oxygen, as one would expect, since argon has a larger molecular weight than oxygen.

Argon has three stable isotopes of mass numbers 36, 38 and 40, which occur in a relative abundance in the atmosphere in the ratios 338:63:100,000.

Argon is present in atmospheric air in a concentration of 0.934 percent by volume or 1.25 percent by weight. Since the boiling point of argon lies between that of liquid oxygen and that of liquid nitrogen (slightly closer to that of liquid oxygen), a crude grade of argon (90 to 95 percent pure) can be obtained by adding a small auxiliary argon-recovery column in an air-separation plant. Argon is delivered either as a gas under high pressure, or as a liquid at low temperature.

Argon is a gas in normal atmospheric conditions (15°C and 760 mm Hg). It is a colorless, odorless and tasteless gas. Perfect physical and chemical stability distinguish it. It is a nontoxic, nonflammable gas. By displacing the oxygen in the air, it may have harmful effects on organism, by reducing the partial pressure of oxygen and acting as an asphyxiant.

Owing to its chemical inertness at elevated temperatures, argon is employed for welding in inert gas atmospheres. Argon, either pure or containing traces of carbon dioxide, oxygen, hydrogen and helium, is the most widely used gas in welding applications involving mild and stainless steels, aluminum and light alloys, magnesium, titanium, etc.

Argon is also employed in metallurgy for heat treatment in a protective atmosphere, notably for annealing of high carbon steels, for which decarburization is to be avoided. It serves as a carrier gas for silane in the deposition and epitaxial growth of silicon.

Table 3.1 Thermophysical Properties of Cryogenics

Air
dew point = 82K

| | Helium | Hydrogen | Neon | Nitrogen | Argon | Oxygen | Methane | Krypton | Xenon | Ethylene | Ethane | Solid CO ₂ |
|---|---------------|----------------|----------------|----------------|----------------|----------------|-----------------|-----------------|-----------------|-------------------------------|-------------------------------|-------------------------|
| Chemical Symbol | He | H ₂ | Ne | N ₂ | Ar | O ₂ | CH ₄ | Kr | Xe | C ₂ H ₄ | C ₂ H ₆ | CO ₂ |
| Molecular Weight | 4 | 2 | 20 | 28 | 40 | 32 | 16 | 84 | 131 | 28 | 30 | 44 |
| Saturation temperature (boiling point) at 1 bar, K (°C) | 4.2 (-269) | 20.3 (-253) | 27.1 (-246) | 77.4 (-196) | 87.3 (-186) | 90.2 (-183) | 111.7 (-161) | 121.4 (-152) | 164.1 (-109) | 169.3 (-104) | 184.6 (-89) | 195 (-78) (sublimes) |
| Freezing temperature, K (°C) | - | 14.1 (-259) | 24.5 (-249) | 63.3 (-210) | 84.0 (-189) | 54.8 (-219) | 90.6 (-183) | 104.2 (-169) | 133.2 (-140) | 104.2 (-169) | 89.9 (-183) | (-56.6 at 5.27 bar) |
| Critical temperature, K (°C) | 5 (-268) | 33 (-240) | 44 (-229) | 126 (-147) | 151 (-122) | 154 (-119) | 191 (-82) | 210 (-63) | 290 (+17) | 283 (+10) | 305 (+32) | 304 (+31) |
| Critical pressure, bar | 2.3 | 13.4 | 27.8 | 34.5 | 49.5 | 51.4 | 47 | 56 | 60 | 52.5 | 49.7 | 73.8 |
| Expansion ratio - increase in volume as liquid at 1 bar boils to gas at 1 bar, 15°C | 738 | 826 | 1417 | 678 | 820 | 843 | 626 | 677 | 556 | 489 | 437 | 812 (solid-gas) |
| Density of saturated liquid at 1 bar (kg m ⁻³) | 125 | 70 | 1200 | 804 | 1390 | 1142 | 424 | 2400 | 3100 | 565 | 546 | 1513 (solid) |
| Relative gas density (referenced to dry air at 1 bar, 15°C, density 1.21 kg m ⁻³) | 0.14 | 0.07 | 0.70 | 0.98 | 1.40 | 1.12 | 0.56 | 2.93 | 4.61 | 0.97 | 1.05 | 1.54 |
| Latent heat of vaporisation (cooling potential of phase change) (hg, kJ kg ⁻¹) | 23.9 | 451.9 | 87.0 | 199.2 | 162.7 | 212.9 | 577.4 | 108.0 | 96.2 | 483.4 | 488.3 | 654 (solid-vap) |
| Fire/explosion hazard | no | flammable | no | no | no | yes | flammable | no | no | flammable | flammable | no |
| Air liquefaction hazard | yes | yes | yes | yes | no | no | no | no | no | no | no | no |

Note: With the exception of liquid oxygen which is light blue all the liquid cryogenics are colourless.

With the exception of C₂H₄ and C₂H₆ which have a slight anaesthetic effect and CO₂ which is mildly toxic (TLV 5000 ppm) all the cryogenics listed are considered non-toxic

3.2.2 Thermodynamic Properties

The state of a substance at any instant is determined by its thermodynamic properties. These properties include pressure (P), temperature (T), volume (V), internal energy (U), enthalpy (H) and entropy (S). For a pure substance in equilibrium, that is a substance of uniform and invariant chemical composition not undergoing any change, the thermodynamic state is uniquely defined by two properties only. It follows that any other (dependent) property must be a function of the chosen pair of independent properties and can be determined accordingly. This is known as the two-property rule. For the special case of saturation conditions where two phases coexist, pressure and temperature are dependent. However, the two-property rule still applies since in order to fully define the thermodynamic state the relative proportions of the phases is required (the dryness fraction) which is therefore effectively an additional property.

The relationship between properties may be presented graphically, as equations (equations of state) or in the form of tables. In the special case of a substance that approximates to an ideal gas, the relationship between thermodynamic properties is expressed by a simple equation of state that can be derived from kinetic theory. However, in general, the equation of state for a real substance is much more complicated than this and must be derived empirically. Such equations are usually presented as computer codes that may then be used to generate property diagrams and tables. In practice, property diagrams and tables are usually preferred unless the behavior of the real substances can be approximated as that of an ideal gas.

Throughout this section, the word "data" is used to refer to experimental measurements. The term "formulation" refers to the equation or equations necessary to calculate fluid properties from correlation. The term "fundamental equation" is used to describe the equation of state used in several methods of developing thermodynamic property formulations. The form of the fundamental equation used in the center for Applied Thermodynamic Studies is a dimensionless potential function

$$\alpha(\delta, \tau) = \alpha^{\circ}(\delta, \tau) + \bar{\alpha}(\delta, \tau) \quad (3-1)$$

where α° is the dimensionless Helmholtz energy for the ideal gas, $\tau = T_c / T$, $\delta = \rho/\rho_c$ and $\bar{\alpha}$ is the real fluid contribution to the dimensionless Helmholtz energy, which is given by

$$\bar{\alpha}(\delta, \tau) = \sum_{i=1}^k N_k \delta^i \tau^j \exp(-\gamma \delta^\lambda) \quad (3-2)$$

where $\gamma = 0$ if $\lambda = 0$ and $\gamma = 1$ if $\lambda > 0$. The value of j is generally expected to be greater than zero, and i and λ are integers greater than or equal to zero.

The primary data sets that are required for determining the fundamental equation are the P - ρ - T data and the ideal gas heat capacity, $C_p^\circ(T)$ to define the ideal gas properties. Vapor pressure and coexistence density data are required to define phase equilibrium condition, consistent with the Maxwell criterion.

It is generally preferable to select the terms to be used in Equation (3-2) based on the statistical significance of each term and the statistical analysis of the overall equation. An excellent procedure is the stepwise least-squares technique with a search and selection procedure introduced by Wagner (1974) and modified for use on equations of state by de Reuck and Armstrong (1979). The selection procedure selects an optimum group of terms from a proposed bank of terms. At the center for Applied Thermodynamic Studies, a bank of 100 terms has been used from the following range of i , j and λ .

With $\lambda = 0$, $i = 1$ to 6 (integers), $j = 0.25$ to 7 (0.25 increments);
with $\lambda = 2$ to 6 (integers), $i = 1$ to 8 (integers), $j = 1$ to 24 (integers).

Since all properties may be obtained from a fundamental equation as derivative functions, computer codes have been written which calculate properties for all of the formulations using the fundamental equation (3-1) with equation (3-2) used for real gas contribution with any of values of i , j and λ within the bounds listed above. Table 3.2 includes references to the equations of state used for the formulations of selected cryogenic fluids.

The fundamental equation is usually developed to accurately represent the phase equilibrium data. Saturated liquid and saturated vapor properties are calculated iteratively using the Maxwell criterion. However, in some cases it may be preferable to define the phase equilibrium states with a vapor pressure equation and calculate the saturation densities as a function of saturation temperature and vapor pressure.

The use of independent function to define coexistence properties introduces thermodynamic inconsistencies in the calculated properties. It is, therefore desirable for the fundamental equation to adhere closely to the Maxwell criterion.

Table 3.2 Recommended Formulations for Selected Cryogenic Fluids

| Cryogenic fluid | Reference | Equation of state | No. of Terms | Accuracy (% ρ) | Temp. range, K | Maximum pressure, Mpa |
|-----------------|-------------------------|-------------------|--------------|----------------------|----------------|-----------------------|
| Nitrogen | Jacobsen, et al. (1986) | 3-1,3-2 | 28 | 0.1 | 63-2000 | 1000 |
| Oxygen | Wagner, et al. (1986) | 3-1,3-2 | 32 | 0.1 | 55-350 | 80 |
| Argon | Stewart, et al. (1989) | 3-1,3-2 | 28 | 0.1 | 84-1200 | 1000 |

The function used for calculating pressure, compressibility factor, internal energy, enthalpy, entropy, isochoric heat capacity, isobaric heat capacity, Gibbs energy, and the velocity of sound from equation (3-1) are given as Equations (3-3)-(3-11). These functions were used in calculating the monograph tables of thermodynamic properties of selected cryogenic fluids.

The compressibility factor is given by the equations

$$Z = P/(\rho RT) = 1 + \delta \left(\frac{\partial \bar{\alpha}}{\partial \delta} \right) \quad (3-3)$$

and

$$P/P_c = \left\{ \delta / (\tau Z_c) \right\} \left\{ 1 + \left(\frac{\partial \bar{\alpha}}{\partial \delta} \right) \right\} \quad (3-4)$$

Similarly,

$$U/(RT) = \tau \{ (\partial \alpha^o / \partial \tau) + (\partial \bar{\alpha} / \partial \tau) \}, \quad (3-5)$$

$$S/R = \tau \{ (\partial \alpha^o / \partial \tau) + (\partial \bar{\alpha} / \partial \tau) \} - \alpha^o - \bar{\alpha}, \quad (3-6)$$

$$H/(RT) = \tau \{ (\partial \alpha^o / \partial \tau) + (\partial \bar{\alpha} / \partial \tau) \} + \delta (\partial \bar{\alpha} / \partial \delta) + 1, \quad (3-7)$$

$$G/(RT) = 1 + \alpha^o + \bar{\alpha} + \delta (\partial \bar{\alpha} / \partial \delta), \quad (3-8)$$

$$C_v/R = -\tau^2 \{ (\partial^2 \alpha^o / \partial \tau^2) + (\partial^2 \bar{\alpha} / \partial \tau^2) \}, \quad (3-9)$$

$$C_p/R = (C_v/R) + \left[\frac{\{ 1 + \delta (\partial \bar{\alpha} / \partial \delta) - \delta \tau (\partial^2 \bar{\alpha} / \partial \delta \partial \tau) \}}{\{ 1 + 2\delta (\partial \bar{\alpha} / \partial \delta) + \delta^2 (\partial^2 \bar{\alpha} / \partial \delta^2) \}} \right]^2, \quad (3-10)$$

$$W^2/(RT) = \frac{1 + 2\delta (\partial \bar{\alpha} / \partial \delta) + \delta^2 (\partial^2 \bar{\alpha} / \partial \delta^2) - \left[\{ 1 + \delta (\partial \bar{\alpha} / \partial \delta) - \delta \tau (\partial^2 \bar{\alpha} / \partial \delta \partial \tau) \}^2 / \{ \tau^2 (\partial^2 \alpha^o / \partial \tau^2) + \tau^2 (\partial^2 \bar{\alpha} / \partial \tau^2) \}}}{}, \quad (3-11)$$

The densities for the saturated liquid and saturated vapor were calculated iteratively from the fundamental equation. The derived properties for saturation states were calculated as functions of temperature and density using standard thermodynamic relations. Table entries for the liquid-vapor saturation table were calculated using the vapor pressure equation to determine P_{sat} at the table value of T_{sat} . The vapor pressure correlation by Wagner (1973) is a thorough study and it is accurate representation of published vapor pressure data.

The numerical values of properties listed in the monograph tables, and expressed in identical units throughout this application, are the database of Gas Encyclopaedia (L' AIR LIQUIDE), which are derived from interpolation, extrapolation, or unit conversion computer programs, employing the data contained in the bibliographic references. These properties are given to the fourth decimal at least in order to facilitate interpolation.

3.2.3 Transport Properties

The determination of viscosity, one of the fundamental magnitudes characterizing the physical properties of real gases, is a rather pressing problem. Reliable data on the viscosity are no less important for solving some practical problems than knowledge of thermodynamic properties, and they can better explain the processes of molecular transfer in gases. During recent years, an increasing number of studies have discussed the transport properties of substances, but the problem has not been solved. The physical entity of the transfer coefficients is more complex than that of the thermodynamic functions, and these coefficients have not been sufficiently studied either experimentally or theoretically.

The viscosity of compressed gases has been studied more than either thermal conductivity or diffusion, but in most cases, experimental data on viscosity cover a narrow range of parameters. Dynamic viscosity of cryogenic liquids is an important parameter in deep-freeze installations. Nevertheless, viscosity of that liquids for temperatures from triple point to critical point at sufficiently high pressure has so far not been tabulated. Therefore, great importance is attached to methods with which it is possible to reliably calculate the viscosity over wide ranges of temperature and pressure of interest in industry from the limited experimental data.

The transport properties of selected cryogens in GASPAK programme are from the National Bureau of Standards Technical Note 1097, dated May 1986 by R. D. McCarty.

The equation obtained for calculating the viscosity and thermal conductivity of selected cryogenic fluids in this application can be written as follows:

For gaseous nitrogen

$$\eta_{P,T} = \eta_T + 1383\rho + 2383\rho^2 + 16075\rho^3 - 32888\rho^4 + 41021\rho^5, \quad (3-12)$$

$$\lambda_{P,T} = \lambda_T + 3074\rho + 15767\rho^2 - 22696\rho^3 + 28503\rho^4, \quad (3-13)$$

for gaseous oxygen

$$\eta_{P,T} = \eta_T + 1199\rho + 5201\rho^2 - 5811\rho^3 + 8914\rho^4, \quad (3-14)$$

$$\lambda_{P,T} = \lambda_T + 2545\rho + 19276\rho^2 - 43323\rho^3 + 47784\rho^4 - 15630\rho^5, \quad (3-15)$$

for gaseous argon

$$\eta_{P,T} = \eta_T + 1150\rho + 4290\rho^2 - 3345\rho^3 + 3683\rho^4, \quad (3-16)$$

$$\lambda_{P,T} = \lambda_T + 1950\rho + 4936\rho^2 - 4834\rho^3 + 3371\rho^4, \quad (3-17)$$

where density is given in kg/dm^3 , viscosity in 10^{-8} newton.sec/ cm^2 and thermal conductivity in 10^{-8} kW/ m°C . From equation (3-12), which holds over the range of densities $\rho = 0 - 0.72 \text{ kg/dm}^3$, the viscosity values of gaseous nitrogen up to 1300 K and 1000 bar were calculated with an accuracy of $\pm 2\%$. The viscosity of oxygen that calculated from equation (3-14) is given for rounded off pressures and temperatures in the ranges 100-1300 K and 1-1000 bar. Although the data on the viscosity of oxygen under atmospheric pressure are not less accurate than similar values for nitrogen but they are accurate within $\pm 3\%$. The accuracy of viscosity values of argon that calculated from equation (3-16) for 90-1300 K at pressure up to 1000 bar in the range of 0-1.15 kg/dm^3 is $\pm 2\%$.

The great interest shown in thermal conductivity is due to the necessity of designing various heat-exchange installations with liquid and gas coolants. Much attention has lately been paid to the study of the thermal conductivity of gases and liquids over wide ranges of temperature and pressure. The thermal conductivity of selected gases calculated from equation (3-13), (3-15) and (3-17) respectively for temperatures up to 1300 K and pressure up to 1000 bar are correct for the range of $\rho = 0 - 0.7 \text{ kg/dm}^3$, $\rho = 0 - 1.2 \text{ kg/dm}^3$ and $\rho = 0 - 1.4 \text{ kg/dm}^3$ respectively. The error in those calculated values of thermal conductivity is not exceeding 4%.

An expression for excess viscosity of gaseous nitrogen was formed for $\rho = 0-0.72 \text{ kg/dm}^3$. When using this expression to extrapolate to $\rho = 0.9 \text{ kg/dm}^3$, calculated values of $\Delta\eta$ turn out to be considerably lower than our reference values. The viscosity of liquid nitrogen should be governed by equation (3-12) at densities below 0.65 kg/dm^3 . This equation was only used for temperatures above 107 K, since at lower temperatures the density of liquid nitrogen exceeds 0.65 kg/dm^3 .

For $\rho = 0.65-0.90 \text{ kg/dm}^3$, the reference data is described with an error of less than 1% by

$$\eta_{P,T} = \eta_T + 52.09 + 253.4(\rho-0.65) + 1638(\rho-0.65)^2 - 29438(\rho-0.65)^3 + 283350(\rho-0.65)^4 - 471070(\rho-0.65)^5, \quad (3-18)$$

in which viscosity is expressed in viscosity in $10^{-6} \text{ newton.sec/cm}^2$ and density in kg/dm^3 .

The function $\Delta\eta = f(\rho)$ for oxygen increases sharply at densities above 1.5 kg/dm^3 and cannot be described by density extrapolation of equation (3-14). Viscosity of liquid oxygen at densities lower than 0.92 kg/dm^3 can be calculated by equation (3-14). We only used it for temperatures above 127 K, since at lower temperatures the density of liquid oxygen exceeds 0.92 kg/dm^3 even on saturation curve. For $\rho = 0.92-1.26 \text{ kg/dm}^3$, we obtained the following formula in same units as in equation (3-18) describing the reference curve of oxygen with an error of up to 1.5%:

$$\eta_{P,T} = \eta_T + 73.66 + 237.8(\rho-0.92) + 486(\rho-0.92)^2 + 10695(\rho-0.92)^3 - 79367(\rho-0.92)^4 + 208570(\rho-0.92)^5. \quad (3-19)$$

The viscosity of liquid argon at densities lower than 1.05 kg/dm^3 (i.e., at many points for temperatures above 132 K) can be calculated by equation (3-16). At densities between 1.05 and 1.45 kg/dm^3 reference values of excess viscosity of liquid argon are represented in same units as above cryogenes with an error of less than 1% by

$$\eta_{P,T} = \eta_T + 65.42 + 161.5(\rho-1.05) + 225(\rho-1.05)^2 + 7503(\rho-1.05)^3 - 33918(\rho-1.05)^4 + 56905(\rho-1.05)^5. \quad (3-20)$$

The empirical conductivity of gaseous air components are generalized over wide range of temperatures and densities in $(\Delta\lambda, \rho)$ coordinates, and resulting curves are described very accurately by polynomials up to the fourth or fifth power of density. Unlike formulas for calculating viscosity, those for determining excess conductivity of gaseous nitrogen and argon agree satisfactorily (even when extrapolated with respect to densities) with data for liquid at all densities. The derivative $d(\Delta\lambda)/d\rho$ does not start to increase sharply above 2.5 critical densities, and therefore density extrapolation of earlier formulas does not deviate substantially from empirical data.

The absence of sharp changes in curvature of reference curves $\Delta\lambda = f(\rho)$ for nitrogen and argon enabled the curves to be applied over a wide range of densities, including subcritical densities, in the following form containing five terms in all:

for nitrogen

$$\lambda_{P,T} = \lambda_T + 29.46\rho + 175.67\rho^2 - 305.78\rho^3 + 420.06\rho^4 - 79.16\rho^5, \quad (3-21)$$

for argon

$$\lambda_{P,T} = \lambda_T + 18.52\rho + 57.98\rho^2 - 71.53\rho^3 + 57.18\rho^4 - 7.52\rho^5, \quad (3-22)$$

where λ is expressed in 10^{-6} kW/m²°C. Equation (3-21) and (3-22) describe reference curves for densities of 0.15-0.9 and 0.20-1.45 kg/dm³ with errors of less than 0.20 and 0.35% respectively. We also used equation (3-15) to calculate conductivity of liquid oxygen at pressures of up to 500 bar, since for fixed pressure, liquid density decreases with rise in temperature. To calculate conductivity on 75-90 K isotherms at pressures of up to 500 bar, we can use equation (3-15) up to $\rho = 1.27$ kg/dm³.

3.3 Cryogenic Transfer Systems

Choosing the proper type of line to transport a cryogenic liquid requires a thorough analysis of the design objectives. A cryogenic fluid transfer line is generally one of three types:

1. uninsulated lines,
2. porous-insulated lines, and
3. vacuum-insulated lines.

All of these systems share somewhat several typical design problems associated with cryogenic liquid transfer. One class of difficulties results from cooling the system down from ambient to cryogenic temperature. Evidence of cooldown is in the form of two-phase flow, thermal contraction, and line bowing. Thermal contraction of a transfer line must not result in contact between the inner and outer lines, a condition most frequently encountered at changes in direction of the transfer lines.

3.3.1 Uninsulated Transfer Lines

Frequently, it is more economical to transport a cryogen through an uninsulated line than spend the time and money to insulate the line from heat inleak. An uninsulated pipe is generally employed for short transfer distances and for short or infrequent use periods.

In an uninsulated line, cooldown costs are low and frost due to sublimed water vapor quickly forms on the pipe to provide some insulation. The heat flux to the transfer line may be estimated from the convective heat-transfer rate equation including radiation,

$$Q/A = \bar{h}_c(T_a - T_f) + e_f \sigma (T_a^4 - T_f^4). \quad (3-23)$$

where the emissivity of the frost (e_f) may be taken as 0.92 and T_a and T_f are the absolute temperatures in Kelvin of the surrounding air and the frost surface. The mean heat transfer coefficient can be estimated for free convection only in this programme by one of the following correlations:

1. For free convection, laminar flow, $(Gr)(Pr) < 2 \times 10^9$

$$Nu = \bar{h}_c D / k_f = 0.540 [Pr / (0.952 + Pr)] [(Gr)(Pr)]^{1/4}, \quad (3-24)$$

2. For free convection, turbulent flow, $(Gr)(Pr) > 2 \times 10^9$

$$Nu = 0.11 [(Gr)(Pr)]^{1/3}, \quad (3-25)$$

where k_f is the mean thermal conductivity of the frost, Pr is the Prandtl number and Gr is the Grashof number. The fluid properties are evaluated at the mean temperature between the ambient temperature and frost surface temperature. The accuracy of these equations is ± 25 percent.

3.3.2 Porous-insulated Lines

Insulations such as glass wool, polystyrene, and polyurethane foam are applied to the bare pipe to reduce heat inleak and have an inexpensive transfer line at the same time. These insulations when properly applied with a vapor barrier may significantly reduce the heat inleak and prove feasible for use with cryogenics at temperatures as low as that of liquid nitrogen. Since water vapor would otherwise diffuse into the insulation and degrade the insulation performance. If no air condensation is present within the insulation, the steady-state heat flux to a porous-insulated line may be determined from

$$Q/A_o = (T_a - T_f) / [(D_o / \bar{k}_t) \ln(D_o / D_i) + (1 / \bar{h}_c)], \quad (3-26)$$

where A_o is the outside heat transfer area of insulation, D_o and D_i the outside and inside insulation layer diameters, respectively, T_a the ambient temperature (K), T_f the fluid temperature (K), \bar{k}_c the mean thermal conductivity of the insulation as shown in table 3.3, and \bar{h}_c the mean convective heat transfer coefficient determined from either equation (3-24) or (3-25).

Table 3.3 Thermal Conductivity for Foam Insulations

| Insulation Type | Density kg/m ³ | Thermal Conductivity k, KJ/s/mK |
|-----------------|------------------------------|------------------------------------|
| Polystyrene | 46 | 3.30×10^{-5} |
| Polystyrene | 39 | 2.60×10^{-5} |
| Polyurethane | 40-60 | 2.70×10^{-5} |
| Foam glass | 136 | 4.18×10^{-5} |

3.3.3 Vacuum-insulated lines

The vacuum-insulated line consists of an inner pipe that carries the cryogenic fluid, and outer concentric pipe that contain the vacuum. The inner line should be made as thin as possible to minimize cooldown losses and the material of construction selected should be compatible with cryogen. Vacuum-jacketed lines are usually designed according to the ASA Code for Pressure Piping. The radiation from the warm surface to cold surface tends to be the dominating mode of heat transfer in vacuum insulation and can be approximated by the modified Stefan-Boltzmann equation.

$$Q_r/A_1 = \sigma F_e F_{1-2} (T_2^4 - T_1^4), \quad (3-27)$$

where Q_r/A_1 is the heat transfer rate by radiation per unit area of inner surface, σ the Stefan-Boltzmann constant, F_e the emissivity factor, and F_{1-2} a configuration factor relating the two surface whose temperatures (K) are T_1 and T_2 . Here subscripts 1 and 2 refer to the inner (colder) and outer (warmer) surfaces, respectively. In this

application, we assume $F_{1-2} = 1$ and the emissivity factor for diffuse radiation for concentric cylinders is given by

$$F_e = \left[\left(\frac{1}{e_1} \right) + \left(\frac{A_1}{A_2} \right) \left(\frac{1}{e_2} - 1 \right) \right]^{-1}, \quad (3-28)$$

where e is the emissivity of the surface and A is the surface area.

3.3.4 Two-Phase Flow in Cryogenic-Fluid Transfer Systems

A phase is simply one of the states of matter and can be a gas, a liquid, or a solid. Multiphase flow is the simultaneous flow of several phases. Two-phase flow is the simplest case of multiphase flow. Vapor-liquid mixtures in cryogenic-fluid transfer systems are referred to as two-phase single-component mixtures.

Because of the even-present problem of heat inleak to a cryogenic-fluid transfer system, some form of two-phase flow is common in these systems. The presence of two-phase flow complicates the problem of predicting such parameters as pressure drop in several ways. First, the flow pattern is often different for vertical, horizontal, and inclined flow. Secondly, several different flow patterns may exist. Third, the flow may be laminar in the liquid phase and turbulent in the vapor phase or any of four combinations may exist. Finally, flow pattern changes along the length of the line if the quality of fluid changes because of heat transfer or pressure drop.

Of the several different types of flow patterns that may exist, seven distinct varieties are apparent as shown in the Baker diagram of Figure 3.2.

In *stratified flow*, the liquid phase flows along the bottom of the pipe with little interference with the vapor phase flowing above. This type of flow occurs when the vapor flow rate is relatively low. As the vapor velocity is increased, the shear force between the two phases becomes large enough that waves are formed in the surface of liquid phase, and *wave flow* results. There may be liquid entrained in the gas. *Slug flow* is attained as greater vapor flow rates cause the waves to reach such proportions that

the entire pipe is filled at intervals with slugs of liquid. These slugs of liquid are separated by regions in which the flow is actually stratified. For relatively high vapor and liquid flow rates, the liquid is forced outward to the pipe wall, and the vapor flows along a central core, so the flow pattern is *annular flow*. The gas core may contain liquid droplets but otherwise the two phases are separate as for stratified and wave flow. At higher vapor velocities, the annular layer of liquid is torn apart by shear forces, and the liquid phase disintegrates into a mist or spray evenly dispersed within the vapor phase; thus, *mist flow* or *dispersed flow* results.

For low-quality flow, the vapor bubbles are formed within the continuous liquid phase, and *bubble flow* is achieved. For horizontal flow, the bubbles are usually concentrated near the top of the pipe, however, in vertical flow, the bubbles may be dispersed throughout the liquid. Increasing the vapor content of the flowing stream causes the bubbles to collect into plugs of vapor, which flow at intervals along the top of the pipe; hence, the name *plug flow* is applied to this flow pattern.

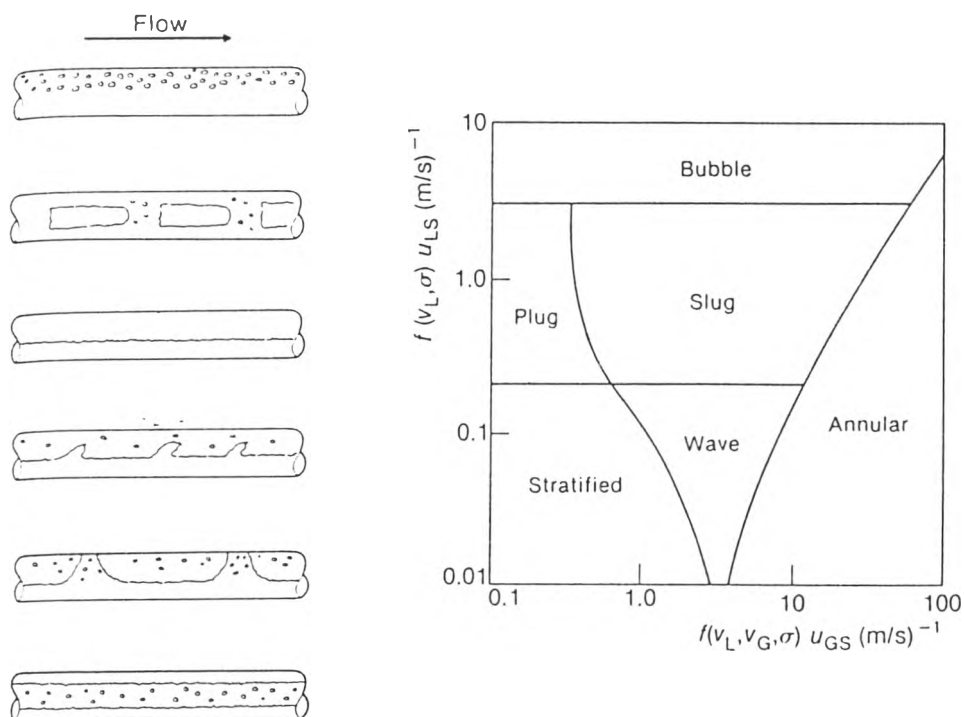


Figure 3.2 Flow patterns and map for horizontal flow

Taitel and Dukler show that the relevant groups governing flow pattern transitions for horizontal flow are Lockhart-Martinelli parameter and one or other of dimensionless groups, depending on the transition. Figure 3.3 demonstrates the Taitel-Dukler map.

Figure 3.4 illustrates the principal flow patterns and the flow pattern map for vertical upflow based on the work of Govier and Aziz. Two of flow patterns, bubble and annular, remain very similar to those obtained with horizontal flow, though with the bubble flow pattern the distribution is of course influenced by the change in pipe inclination. With increasing flow velocity, a breakdown of the slug flow bubbles occurs and leads to an unstable regime in which there is, in wide bore pipes, an oscillatory motion of the liquid upward and downward in the pipe; thus the name *churn flow*. For vertical downflow according to Golan and Stenning, the flow patterns and map are as shown in Figure 3.5.

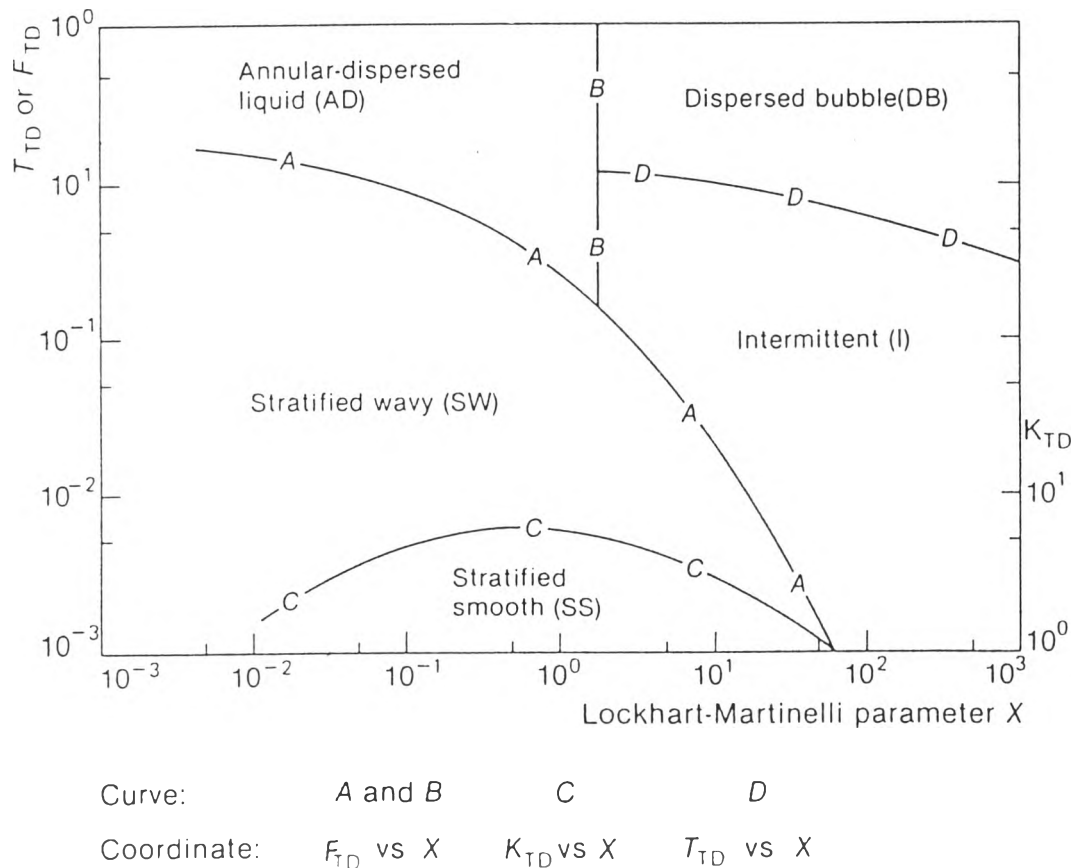


Figure 3.3 Generalized flow pattern map for horizontal flow

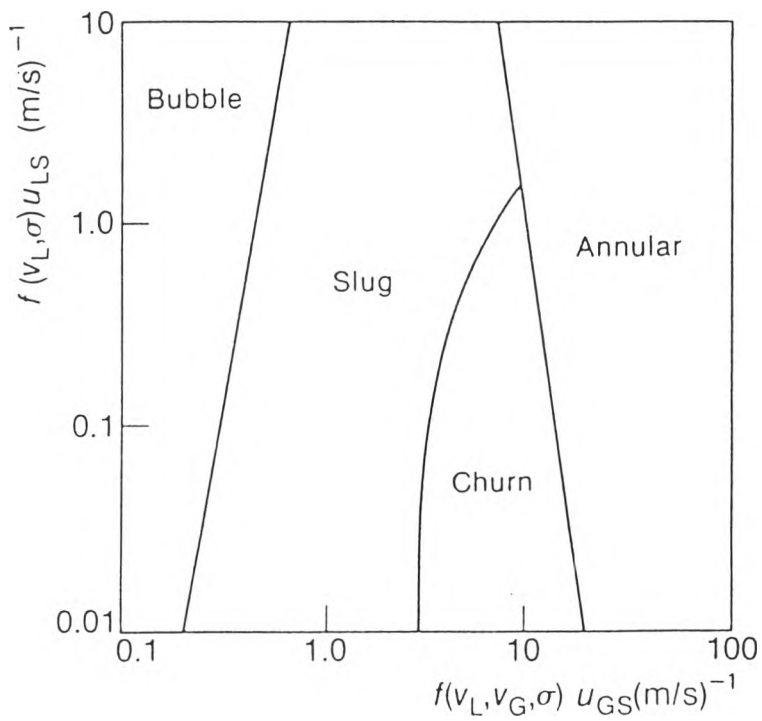
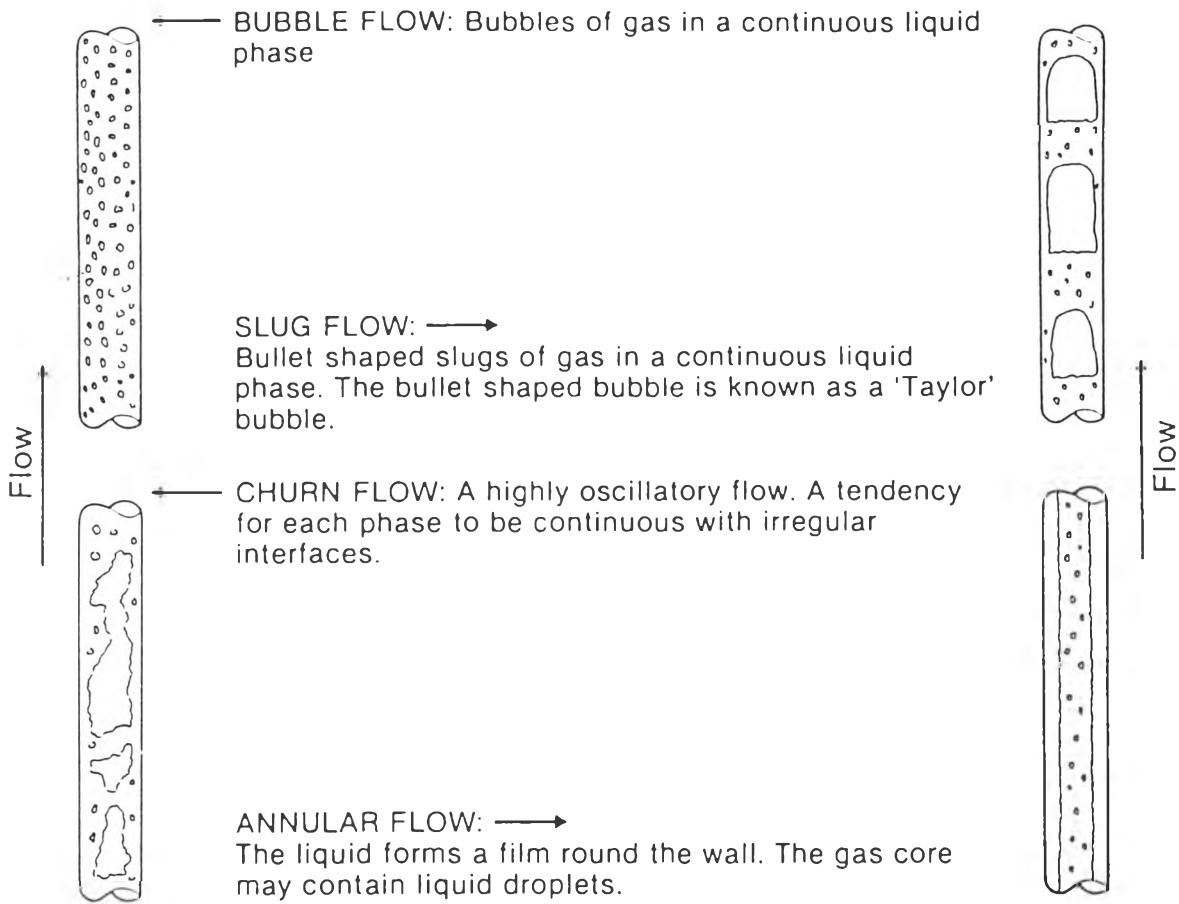


Figure 3.4 Flow patterns and map for vertical upflow

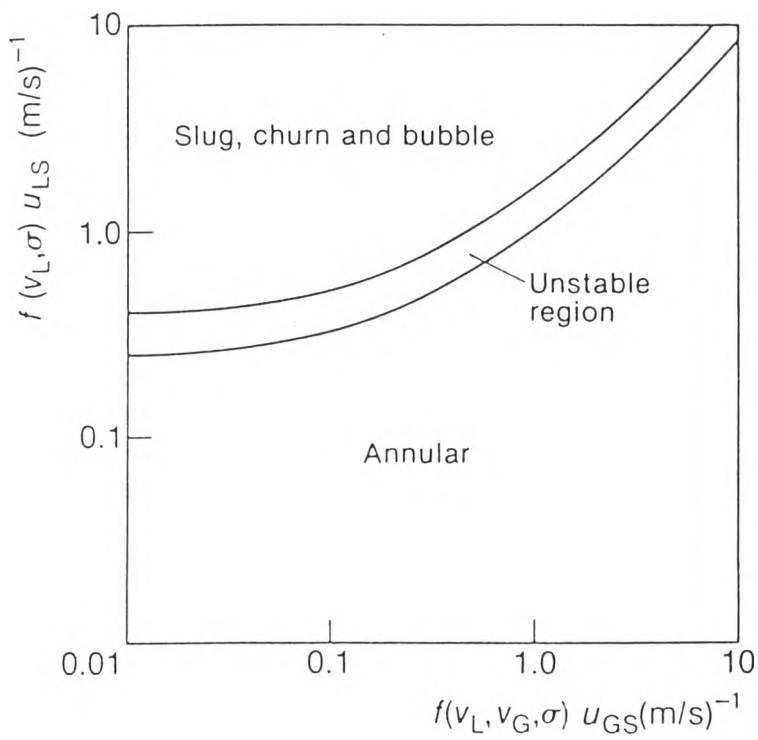
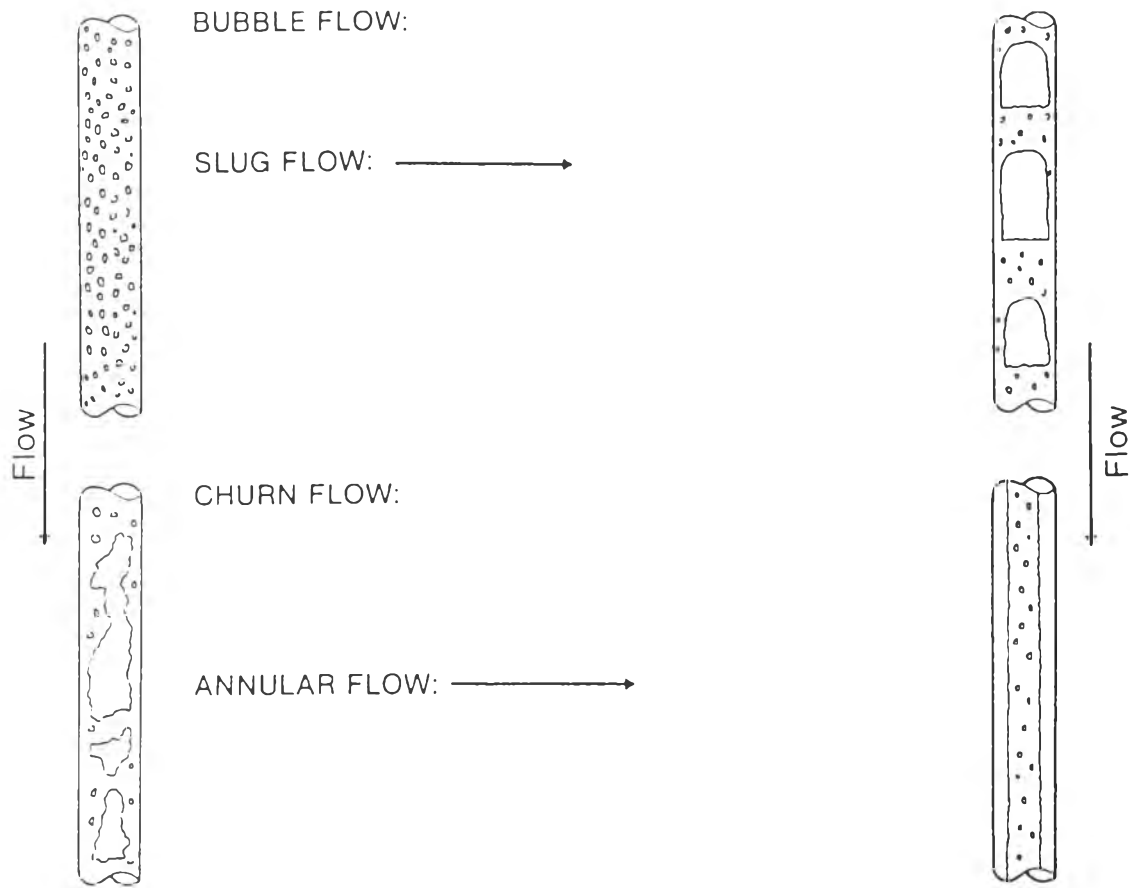


Figure 3.5 Flow patterns and map for vertical downflow.

The design equations presented in this programme attempt to represent these flow patterns. The accuracy with which they do so depends largely on the choice of values for the liquid and gas physical properties. The density, viscosity, specific heat and latent heat of vaporization will have different values at different temperatures and pressures so it is important to be able to use thermodynamic diagrams correctly.

In most cases, the flow within the pipe will be turbulent. This is equivalent to saying that contents of the pipes are well-mixed and uniform temperature. Figure 3.6 illustrates the flow pattern transition from pure subcooled liquids from the bottom of the storage tank to bubbly saturated liquid flow.

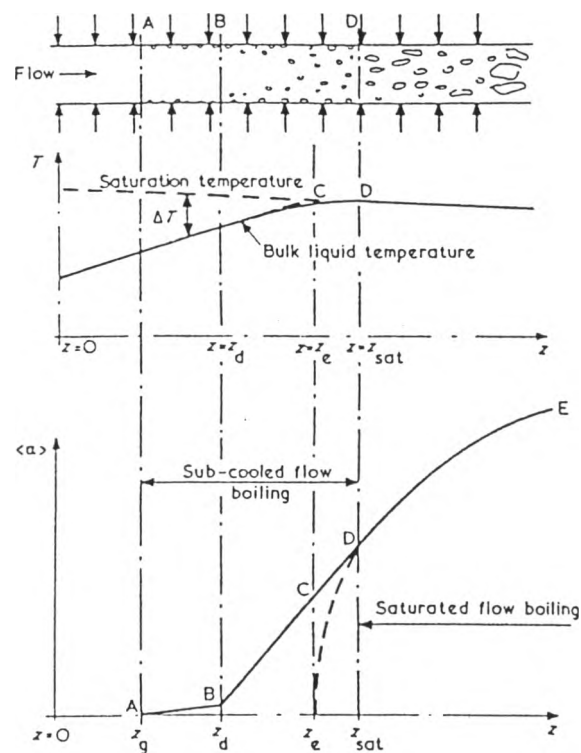


Figure 3.6 Fluid bulk temperature and mean void-fraction distributions in subcooled flow boiling

The following points should be considered:

1. The heat inleak leads to bubble-formation on the pipe wall (A) before saturation conditions are reached (D).
2. The saturation temperature falls over the length of the pipe. T_{sat} is a function of pressure and pressure falls over the length of the pipe to cause the flow.

3. The liquid temperature rises as the heat inleak is absorbed until T_{sat} is reached at the flowing pressure.
4. The amount of vapor or voidage increases along the length of the pipe.
5. The physical properties of liquid and vapor can be determined at (D) if the pressure at that point is known.

The quantity of vapor in the pipe is a variable in the design equations. It can be estimated by the assumptions as follows:

1. The liquid is boiling (saturated) at known $P_{sat}(T_{sat})$;
2. The heat inleak is absorbed by the latent heat of vaporization, that is, a phase change occurs from liquid to gas at constant temperature and pressure;
3. No chemical reaction occurs;
4. It is the steady-state operation;
5. Phase equilibrium is achieved at each pipe length;
6. The exit dryness fractions of each pipe length are the inlet dryness fraction of the next pipe length.

This estimate is called the gas quality or the dryness fraction that is given by

$$x = [(Q/L) \cdot L] / (4.184 \cdot \Delta H \cdot M), \quad (3-29)$$

where (Q/L) is the heat inleak in kJ/s/m calculated from equation (3-23), (3-26), or (3-27), and L is the length of the pipe in metre, ΔH is latent heat of vaporization in kcal/kg, and M is the total mass flow rate which is the sum of the mass flow rates of the phases (QCE343-987, 1987) .

It is strictly only true for the region downstream of (D) in figure 3.6. However, it is used for its simplicity. By if the liquid is always at T_{sat} , it will overestimate the voidage in the region up to D and will therefore lead to an overestimate of the pressure drop.

The gas quality calculation of equation (3-29) is made with data from a point in the pipe, usually the end of the pipe. In practice, there is more value in knowing how the variables change at each end of a system than at each point within the system. The design equations reflect this preference by using the numerical average of the inlet and exit qualities. A better agreement between calculated and actual pressure drops is obtained by using the exit quality in two-phase multiplier equations and shorter pipe segments.

Knowing the pressure drop in a two-phase flow system is of primary interest to the designer in order to establish the pumping load and prescribe the longitudinal variation in pressure necessary to compute the fluid properties along the pipe length. The static pressure drop can be expressed as

$$-\Delta p_{12} = -\Delta p_{f12} - \Delta p_{m12} - \Delta p_{g12} - \Delta p_{f12}, \quad (3-30)$$

where Δp_{12} is used to indicate a pressure rise between point 1 and 2 along a flow path

$$-\Delta p_{12} = \int (dp/dz) \cdot dz, \quad (3-31)$$

Hence, where Z is the length between points 1 and 2. In addition, on the right-hand side of equation (3-30) the pressure drops are the components due to friction, momentum change, gravity, and fitting.

In the designing for two-phase conditions, a major problem is the prediction of effective density of mixture (ρ_m) for use in obtaining the pressure change due to gravity. The gravitational component of the pressure drop in mbar is

$$-\Delta p_{g12} = (g/100) \cdot (\rho_m / \rho_L) \cdot (\sin \theta / v_L) \quad (3-32)$$

where θ is the angle of pipe to horizontal by using the negative sign indicates upflow and v_L are the specific volume ($1/\rho_L$) of liquid.

The volume flow ratio (β) that is normally used to denote the ratio of the gas-volumetric flow rate to total volumetric flow rate can be defined as

$$\beta = (xv_G)/[xv_G+(1-x)v_L], \quad (3-33)$$

where V_G and V_L are the specific volume of gas and liquid respectively.

For the case where the mass dryness fraction varies linearly along a uniform bore pipe and the physical properties remain constant, the average density ($\bar{\rho}_m$) can be obtained (Chisholm, D., 1983)

$$(\bar{\rho}_m/\rho_L) = 1 - C_A [1 - (\bar{\rho}_H/\rho_L)], \quad (3-34)$$

where C_A is the Armand coefficient remains constant along the pipe length that can be obtained from equations as shown in Table 3.4.

Table 3.4 Equations for Armand coefficient

| β | Inclination | Equations |
|---------|-------------|--|
| | Horizontal | $\frac{1}{C_{Ah}} = 0.7 + \frac{0.3}{[1 - 0.7(1 - v_L/v_G)]^{1/2}} \quad (3-35)$ |
| | Vertical | $u_H > \frac{u_{wD}}{(1/C_{Ah}) - 1} \quad C_{Av} = C_{Ah} \quad (3-36)$ |
| | | $u_H < \frac{u_{wD}}{(1/C_{Ah}) - 1} \quad w = 1.4 \left(\frac{v_G}{v_L}\right)^{1/5} \left(1 - \frac{v_L}{v_G}\right)^5 \quad (3-37)$ |
| < 0.9 | | $D > 19 \left[\frac{\sigma v_L}{g(1 - v_L/v_G)} \right]^{1/2} \quad \frac{1}{C_{Av}} = 1 \pm \frac{1.53w}{u_H} \left[\frac{g(v_G - v_L)v_L\sigma}{v_G} \right]^{1/4} \quad (3-38)$ |
| | | $D < 19 \left[\frac{\sigma v_L}{g(1 - v_L/v_G)} \right]^{1/2} \quad \frac{1}{C_{Av}} = 1 \pm \frac{0.35w}{u_H} [gD(1 - v_L/v_G)]^{1/2} \quad (3-39)$ |
| | | Negative sign for downflow |
| | All | $C_A = C_{Ah} - (C_{Av} - C_{Ah}) \left[\frac{\sin 1.8\theta - 0.333 \sin^3 1.8\theta}{0.3} \right] \quad (3-40)$ |
| > 0.9 | | $\frac{1}{C_A} = 1 + \frac{23}{u_H} \left[\frac{\mu_L u_{LS} v_G}{D} \right]^{1/2} \left(1 - \frac{v_L}{v_G}\right) \quad (3-41)$ |

The homogeneous density is

$$\left(\bar{\rho}_H/\rho_L\right) = \left[R_1 R_2 / (R_1 - R_2) \right] \cdot \ln(R_1/R_2), \quad (3-42)$$

where the subscript 1 indicates the upstream conditions during evaporating flow,

$$R = (\rho_H/\rho_L) \quad \text{and} \quad v_H = x v_G + (1-x)v_L.$$

Along a pipe during phase change, The Armand coefficient varies in three different ways as shown in figure 3.7 depending on whether

Case I. $R_C > R_1$, $\beta < 0.9$ and $R_1 > R_C > R_2$, $\beta_C < \beta < 0.9$

The average density, which is given by equation (3-34), can be implemented including with equation (3-42),

where

$$u_{L0} = G v_L, \quad (3-43)$$

$$R_C = u_{L0}/u_t, \quad (3-44)$$

$$R_1 = v_L / [x_i v_G + (1-x_i)v_L], \quad (3-45)$$

$$R_2 = v_L / [x_o v_G + (1-x_o)v_L], \quad (3-46)$$

$$x_C = [(1/R_C) - 1] / [(v_G/v_L) - 1], \quad (3-47)$$

and β_C is determined by calculating equation (3-33) with x_C .

Case II. $R_C > R_1$, $\beta > 0.9$ and $R_1 > R_C > R_2$, $\beta > 0.9$

The average density can be obtained

$$\begin{aligned} \left(\bar{\rho}_m/\rho_L\right) = 1 - C_A + \{ [C_A - \{(1-C_A)/((v_G/v_L)-1)\}] (\bar{\rho}_H/\rho_L) \} \\ - \{(1-C_A)/((v_G/v_L)-1)\} [\frac{1}{2}\{(1/R_2) + (1/R_1)\} - 2]. \end{aligned} \quad (3-48)$$

Case III. $R_2 > R_c$, $\beta < 0.9$ and $R_1 > R_c > R_2$, $\beta < \beta_c$

The average density can be obtained from the set of equation as follows:

$$\left(\bar{\rho}_m / \rho_L \right) = 1 - (1/C_0) [1 - \bar{R}], \quad (3-49)$$

where

$$\bar{R} = \frac{[1 + \{(u_{wD}/u_{LO})(1/C_0)\}][R_1 R_2 / (R_1 - R_2)]}{\ln\{[1 + (C_0 u_{LO}/u_{wD} R_2)] / [1 + (C_0 u_{LO}/u_{wD} R_1)]\}} \quad (3-50)$$

and

$$C_0 = (1/C_A) - (u_{wD}/u_H) \quad (3-51)$$

The generalized correlations for the frictional pressure gradient during two-phase flow in pipes are used in this programme in the sense of not being flow pattern oriented, or restricted to a particular flow pattern. The friction factor is a function of Reynolds number and surface roughness, which covers the complete range of Reynolds number, the Churchill's equation as shown in figure 3.8 is written in computer codes with the absolute roughness of the pipes from table 3.5.

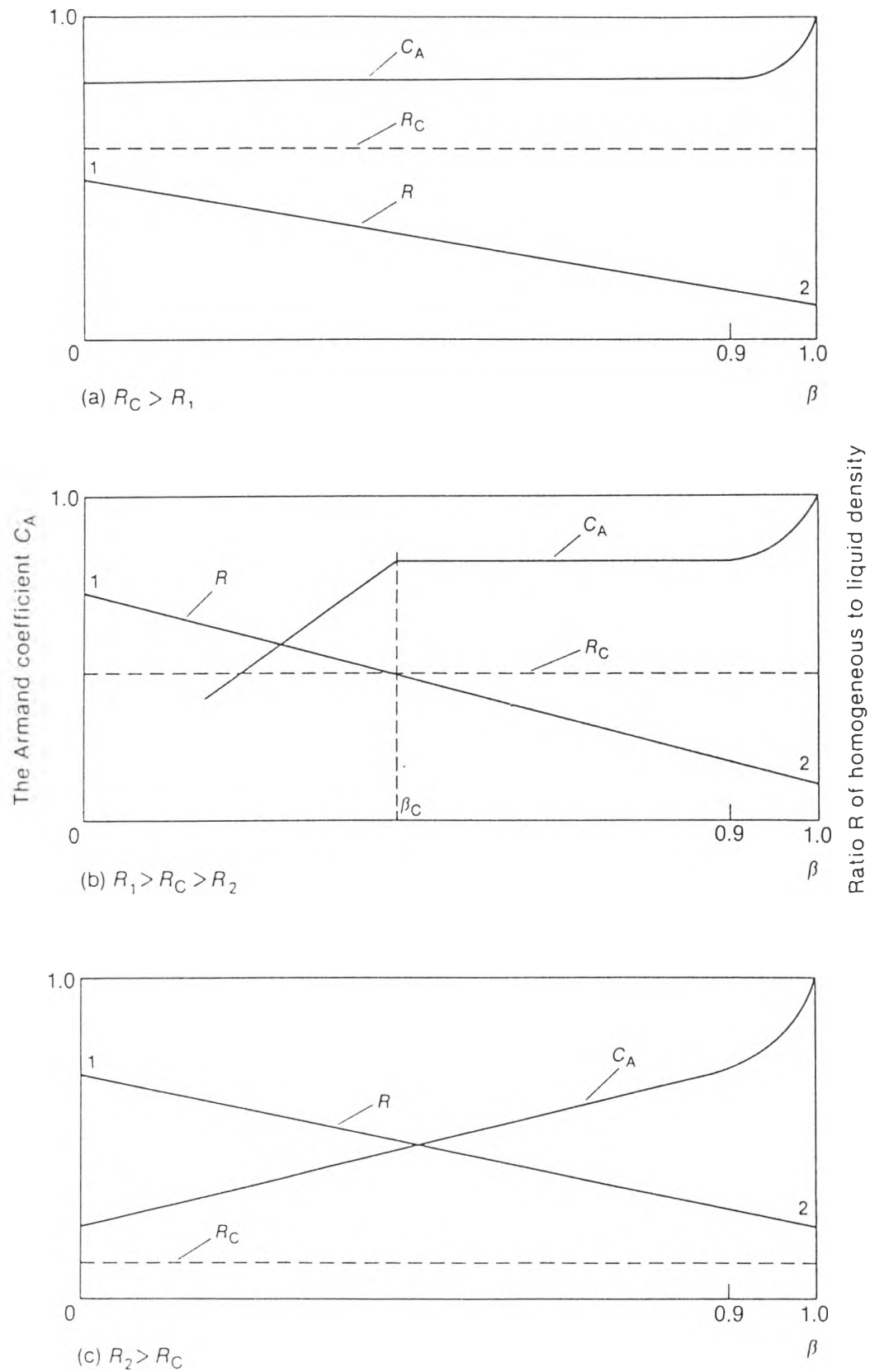


Figure 3.7 Variation of C_A with β and influence of critical R key to relevant equations

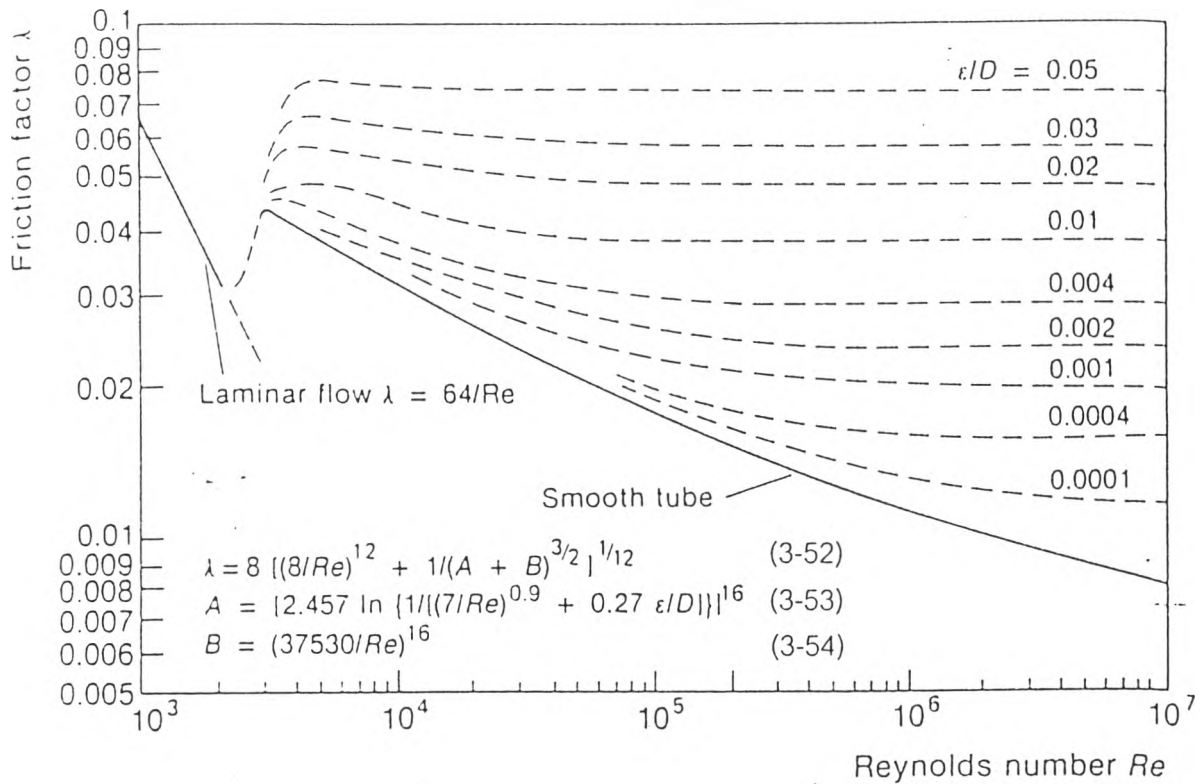


Figure 3.8 Friction factor λ to a base of Reynolds number.

Table 3.5 The value of absolute roughness (ϵ)

| Pipe Material | Absolute roughness (ft) |
|-----------------------------------|-------------------------|
| Drawn tubing | 0.000005 |
| Commercial steel and wrought-iron | 0.00015 |

The corresponding Reynolds numbers are

$$Re_{L0} = G_L D / \eta_L \quad (3-55)$$

$$Re_{G0} = G_G D / \eta_G \quad (3-56)$$

The correlation for the frictional pressure drop is considered in term of two-phase multiplier (ϕ_{FLO}^2) which do not explicitly consider the flow pattern (Chisholm, D., 1973).

$$-\Delta p_{F12} = -Dp_{FLO} \cdot (\varphi_{FLO}^2) \cdot L \quad (3-57)$$

where

$$-Dp_{FLO} = \lambda_{LO} G^2 v_L / 2D \quad (3-58)$$

$$\varphi_{FLO}^2 = 1 + [(\Gamma^2 - 1) \{ (B_F x_o)^{(2-n_B)/2} (1-x_o)^{(2-n_B)/2} + x_o^{(2-n_B)} \}] \quad (3-59)$$

and

$$\Gamma^2 = (\eta_G / \eta_L)^{n_B} \cdot (v_G / v_L) \quad (3-60)$$

$$n_B = \log(\lambda_{LO} / \lambda_{GO}) / \log(Re_{GO} / Re_{LO}) \quad (3-61)$$

Table 3.6 is the recommendation where greater precision is required than given by the method not including the mass velocity correlation.

Table 3.6 Value of B_F for smooth tubes

| Γ | $G / (\text{kg}/(\text{m}^2 \text{ s}))$ | B_F |
|---------------------|--|----------------------------------|
| ≤ 9.5 | ≤ 500 | 4.8 |
| | $500 < G < 1900$ | $2400/G$ |
| | ≥ 1900 | $55/G^{0.5}$ |
| $9.5 < \Gamma < 28$ | ≤ 600 | $520/(\Gamma G^{0.5})$ |
| | > 600 | $21/\Gamma^*$ |
| ≥ 28 | | $\frac{15000}{\Gamma^2 G^{0.5}}$ |

*This B_F corresponds to Lockhart–Martinelli curve.

The predicting equations of the pressure changes due to change in momentum flux are developed for pipe flow,

$$-\Delta p_{M12} = G^2(v_{e0} - v_{ei}) \quad (3-62)$$

where

$$v_{e0}/v_L = 1 + [(v_G/v_L) - 1] \cdot [B_M x_o(1 - x_o) + x_o^2] \quad (3-63)$$

$$v_{ei}/v_L = 1 + [(v_G/v_L) - 1] \cdot [B_M x_i(1 - x_i) + x_i^2] \quad (3-64)$$

and

$$B_M = \{[(1/K)(v_G/v_L)] + (K - 2)\} / [(v_G/v_L) - 1] \quad (3-65)$$

$$K = K_0^{0.28} \quad (3-66)$$

if $X > 1$,

$$K_0 = (v_H/v_L)^{1/2} \quad (3-67)$$

and

$$v_H = x_o v_G + (1 - x_o) v_L \quad (3-68)$$

if $X < 1$,

$$K_0 = (v_G/v_L)^{1/4} \quad (3-69)$$

where the Lockhart-Martinelli parameter (X) can be defined as

$$X = [(1 - x_o)/x_o]^{(2 - n_B)/2} (v_L/v_G)^{1/2} (\eta_L/\eta_G)^{n_B/2} \quad (3-70)$$

The correlations for static pressure drop attributable to fitting are given by

$$-\Delta p_{f12} = -\Delta p_{fLO} \cdot \phi_{fLO}^2 \quad (3-71)$$

where

$$-\Delta p_{fLO} = G^2 v_L K / 2, \quad (3-72)$$

$$\phi_{fLO}^2 = 1 + [((v_G/v_L) - 1) \{ (Bx_o(1-x_o)) + x_o^2 \}]. \quad (3-73)$$

In addition, K is a dimensionless factor defined as the excess head loss in pipe fitting, expressed in velocity heads. In this application, the two K method predicts head losses in that pipe fitting (Hopper, W. B., 1981).

3.4 Gas Piping Systems

Many equations for calculations involving isothermal gas flow in horizontal gas pipelines have been used by the pipeline industry with varying degrees of success over the years. The latest is the rational gas flow formula. For flow in gas pipeline, to take into account differences in elevation, the pressure profile is determined using the rational gas flow formula with J. William Ferguson's elevation correction method (Nayyar, M. L., 1992):

$$P_1^2 - e^s P_2^2 = 76.86 \lambda (ZTGQ^2/D^5)L_e \quad (3-74)$$

where

P_1 = upstream pressure, psia

P_2 = downstream pressure, psia

e^s = elevation correction factor, e is the natural logarithmic base

λ = friction factor is given by the Churchill's equation

Z = compressibility factor

T = absolute gas flowing temperature, °R

G = gas specific gravity

Q = gas flow rate, thousand of cubic feet per hour

D = pipe internal diameter, inch

L = length of pipe segment, miles

H = elevation difference over the segment, feet (positive uphill, negative downhill)

$$s = GH/(26.647TZ) \quad (3-75)$$

$$L_e = \text{effective length, } (e^s - 1)L/s \quad (3-76)$$

The pressure drop of various pipe fittings such as bends, valve etc. can be expressed as number of velocity heads lost which be calculated by equation (3-72).